Supplement of Hydrol. Earth Syst. Sci., 26, 6227–6245, 2022
https://doi.org/10.5194/hess-26-6227-2022-supplement

Hydrology and Earth System Sciences
Open Access

Supplement of

Disentangling scatter in long-term concentration–discharge relationships: the role of event types

Felipe A. Saavedra et al.

Correspondence to: Felipe A. Saavedra (felipe.saavedra@ufz.de)

Supplementary Information

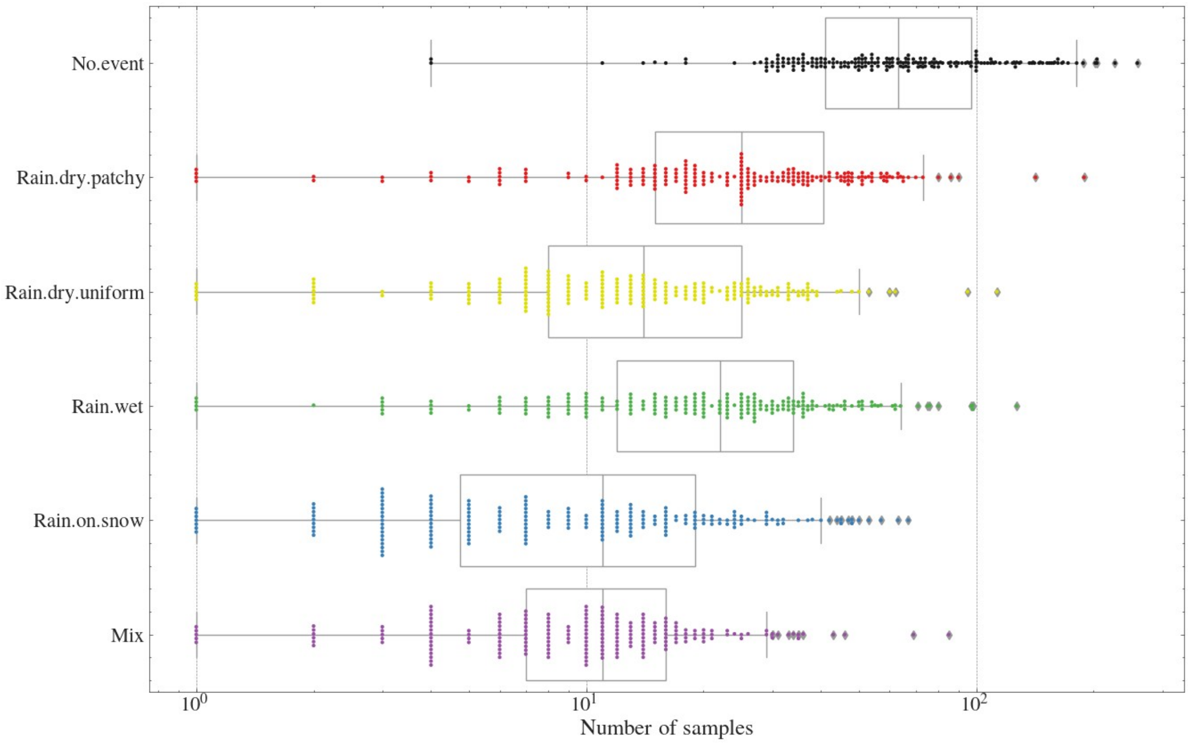

Figure S1. Number of samples in all 184 catchments attributed to each event type. Vertical lines show medians, 5th and 95th percentiles of boxplots.

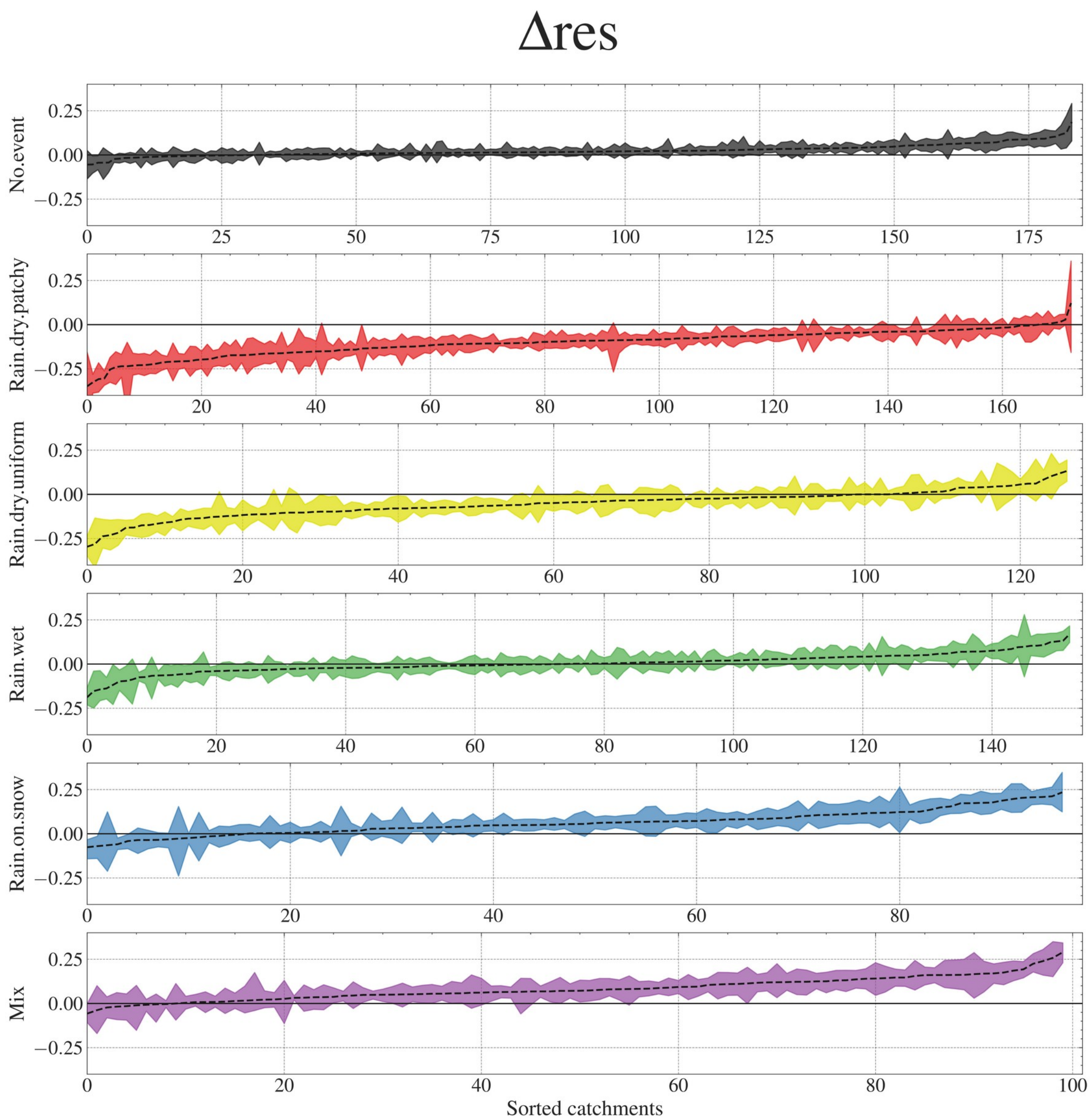

Figure S2. Results of bootstrapping differences of C-Q residuals for different event types and all samples (Δres) 10000 times. Dashed lines show the median bootstrapped differences of residuals (Δres50), and colored bands represent the 25% and 75% percentiles of bootstrapped differences. Catchments are sorted in each subplot based on Δres50 values for better visualization.

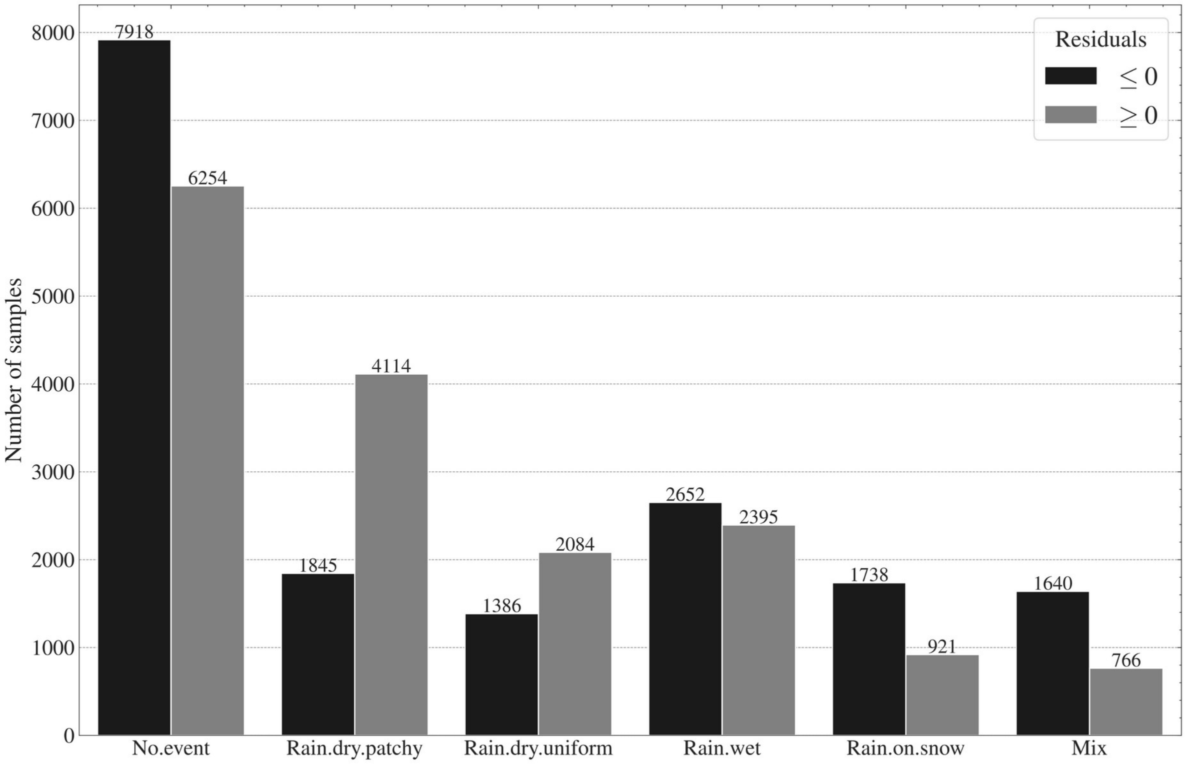

Figure S3: Number of nitrate samples from all catchments with positive and negative residuals for each event type.

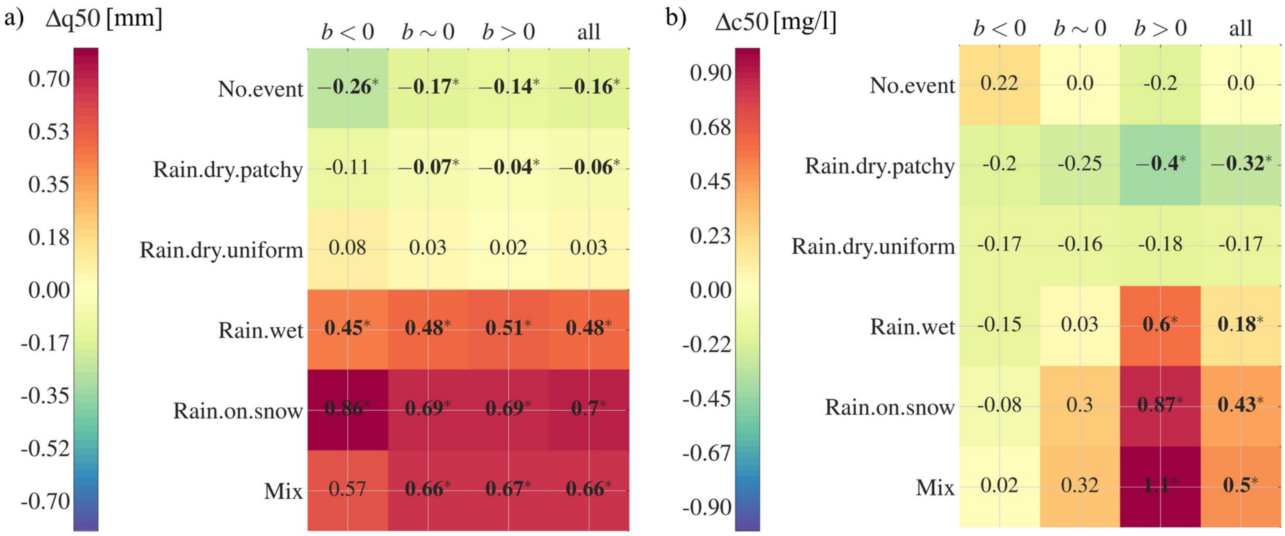

Figure S4. Heatmaps of differences between samples taken during different event types or No.event and all samples (analogous to Figure 5) for a) discharge and b) concentration of nitrate, averaged across different groups of catchments, considering all nitrate data for each event type and No.event. The three first columns of the heatmap correspond to one of the long-term export patterns (i.e., dilution (slope b<0), neutral (slope b~0) and enrichment (slope b>0)) and the fourth column corresponds to all study catchments. Bold font and * indicates significant differences (Kruskal-Wallis test, p<0.05).

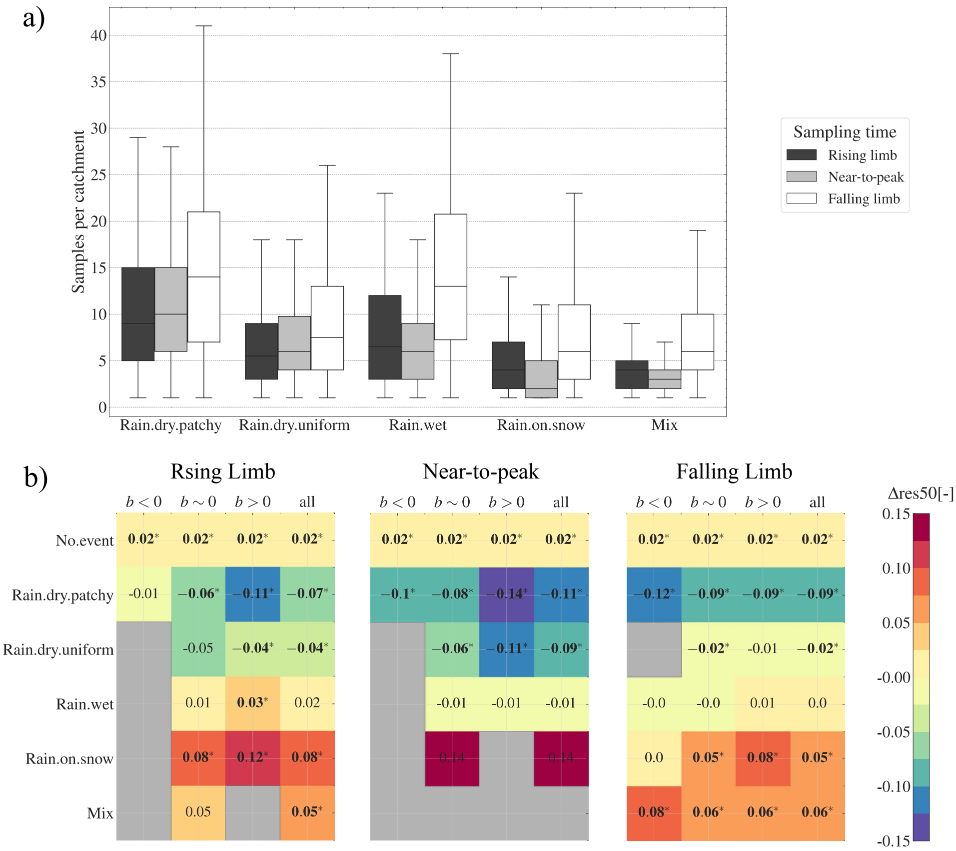

Figure S5. a) Number of samples per catchment per event type corresponding to the samples taken during the rising limb, falling limb, or near to the peak (i.e., samples taken from one day before to one day after the peak of the hydrograph). b) Median deviations of nitrate concentrations from the long-term C-Q relationships (Δres50) for samples taken during the rising limb, falling limb, and near to the peak. Deviations are computed analogously as for Fig. 5 in the main manuscript. The three first columns of the heatmap correspond to one of the long-term export patterns (i.e., dilution (slope b<0), neutral (slope b~0), and enrichment (slope b>0)), and the fourth column corresponds to all study catchments. Bold font and * indicate significant differences (Kruskal-Wallis test, p<0.05) between median deviations across catchments for each event type and median deviation across catchments of all nitrate samples. At least 5 catchments with sufficient data (more than 10 samples per event type) are required to evaluate the significance of the deviations. Gray squares indicate cases where this requirement is not met.

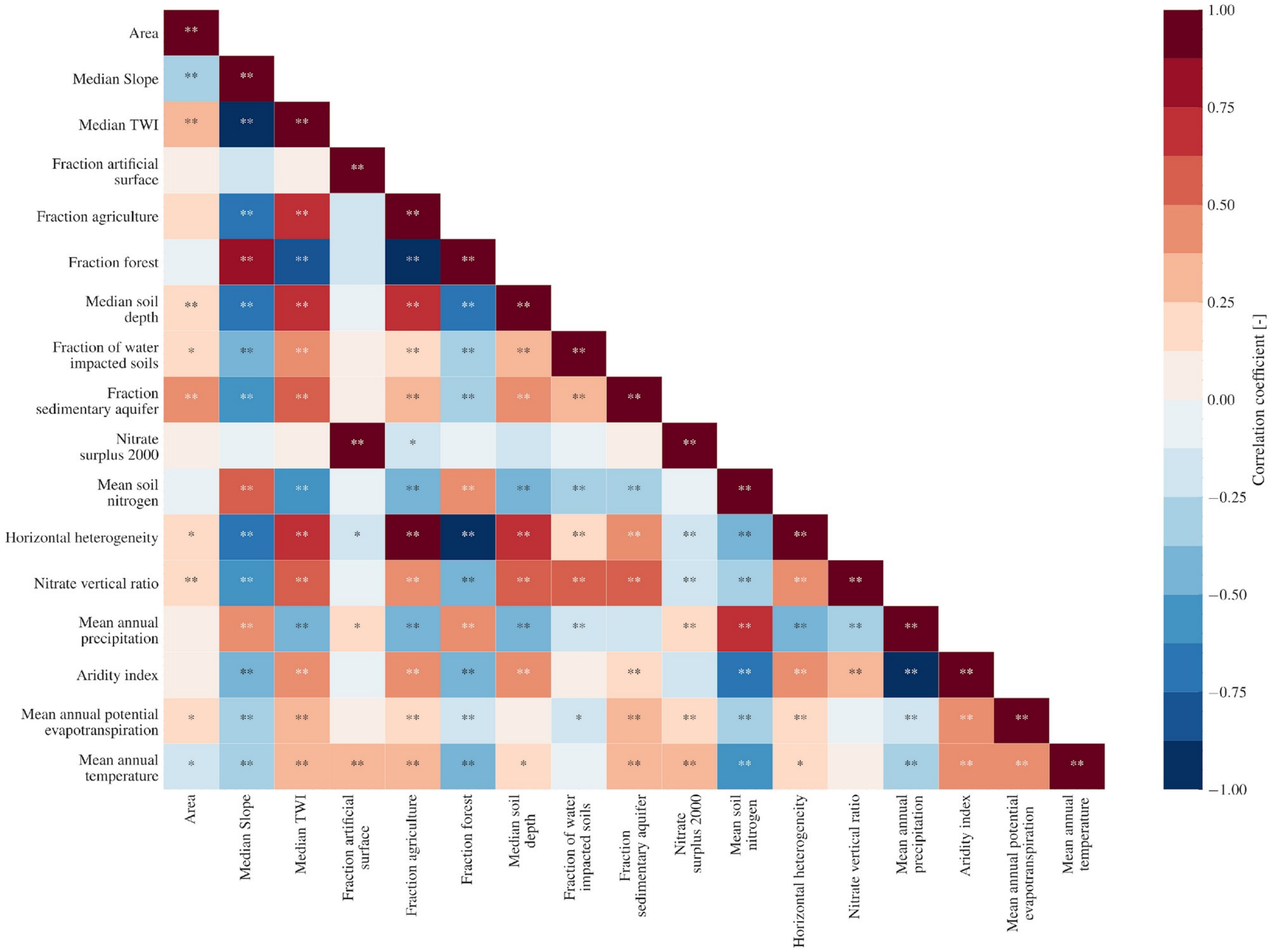

Figure S6. Spearman rank correlation coefficient between catchment descriptors. Significant correlations are indicated as * for p<0.05 and ** for p<0.01.

Table S1: Thresholds and variables used for classification of runoff events (modified from Tarasova et al., 2020).

Layer	Selected indicator	Expression	Thresholds	Performed Split
a) Inducing event	Ratio of event rainfall volume and total event precipitation volume	$\frac{R_{x,y,t}}{P_{x,y,t}}$	0.95	Rainfall vs. Mix or Rain.on.snow
	Normalized spatial covariance of event-averaged snow cover and rainfall	$\frac{\mathrm{cov}_{x,y}(SWE_t, R_t)}{SWE_{x,y,t} \times R_{x,y,t}}$	0	Rain.on.snow vs. Mix
b) Wetness state	Catchment-averaged antecedent soil moisture	$SM_{x,y}(t_0)$	$max(\kappa)$	Wet vs Dry
c) Spatial distribution of mositure	Spatial coefficient of variation of antecedent soil moisture	$\frac{\sqrt{\mathrm{var}_{x,y}(SM_{t_0})}}{SM_{x,y,t}}$	Q_2	Uniform vs Patchy

Note: Input data is grid-based, for each cell (x,y) and time step t during an event the following variables are provided: event rainfall rate $R(x,y,t)$ [mm]; total event precipitation rate $P(x,y,t)$ [mm/day] and snow water equivalent $SWE(x,y,t)$ [mm]. At the beginning of each event (t_0) antecedent soil moisture $SM(x,y,t_0)$ [-] is provided. Q_2 correspond to median value and κ is the curvature of a nonlinear function that describes the relation between event runoff coefficients and simulated soil moisture (Tarasova et al., 2018). Rainfall data was obtained from REGNIE data set (Rauthe et al., 2013). Snow water equivalent and soil moisture were simulated by the mHM model (Samaniego et al 2010; Kumar et al 2013) and provided in Zink et al. (2017).

Table S2: Catchment descriptors used for correlation analysis. (according to Ebeling et al., 2021).

Category	Variable	Unit	Description
Topography	Area	km^2	Catchment area
	Median Slope	$^\circ$	Mean topographic slope of catchment
	Median TWI	-	Mean topographic wetness index
Land Cover	Fraction of agriculture	-	Fraction of agricultural land cover
	Fraction of forest	-	Fraction of forested land cover
Soil & Aquifer	Median soil depth	cm	Median depth to bedrock in the catchment
	Fraction of sedimentary aquifer	-	Fraction of sedimentary aquifer
Nutrient source	Nitrate surplus 2000	$\mathrm{kgN\ ha^{-1} y^{-1}}$	Mean nitrogen surplus per catchment during sampling period (2000–2015) including N surplus on agricultural land and atmospheric deposition on non-agricultural areas
	Horizontal heterogeneity	-	Slope of relative frequency of source areas in classes of flow distances to stream as a proxy for horizontal source heterogeneity
	Nitrate vertical ratio	-	Mean ratio between potential seepage and groundwater NO3-N concentrations as proxy for vertical concentration heterogeneity
Hydrometeorology	Mean annual precipitation	$\mathrm{mm\ y^{-1}}$	Mean annual precipitation for the period 1986–2015
	Mean annual potential evapotranspiration	$\mathrm{mm\ y^{-1}}$	Mean annual potential evapotranspiration for the period 1986–2015
	Aridity index	-	Fraction of mean annual potential evapotranspiration and mean annual precipitation
	Mean annual temperature	$^\circ$C	Mean annual air temperature for the period 1986–2015

References

Ebeling, P., Kumar, R., Weber, M., Knoll, L., Fleckenstein, J. H., and Musolff, A.: Archetypes and Controls of Riverine Nutrient Export Across German Catchments, Water Resources Research, 57, e2020WR028134, https://doi.org/10.1029/2020WR028134, 2021.

Kumar, R., Livneh, B., and Samaniego, L.: Toward computationally efficient large-scale hydrologic predictions with a multiscale regionalization scheme, Water Resources Research, 49, 5700–5714, https://doi.org/10.1002/wrcr.20431, 2013.

Rauthe, M., Steiner, H., Riediger, U., Mazurkiewicz, A., and Gratzki, A.: A Central European precipitation climatology – Part I: Generation and validation of a high-resolution gridded daily data set (HYRAS), Meteorologische Zeitschrift, 235–256, https://doi.org/10.1127/0941-2948/2013/0436, 2013.

Samaniego, L., Kumar, R., and Attinger, S.: Multiscale parameter regionalization of a grid-based hydrologic model at the mesoscale, Water Resources Research, 46, https://doi.org/10.1029/2008WR007327, 2010.

Tarasova, L., Basso, S., Zink, M., and Merz, R.: Exploring Controls on Rainfall-Runoff Events: 1. Time Series-Based Event Separation and Temporal Dynamics of Event Runoff Response in Germany, Water Resources Research, 54, 7711–7732, https://doi.org/10.1029/2018WR022587, 2018.

Tarasova, L., Basso, S., Wendi, D., Viglione, A., Kumar, R., and Merz, R.: A Process-Based Framework to Characterize and Classify Runoff Events: The Event Typology of Germany, Water Resources Research, 56, e2019WR026951, https://doi.org/10.1029/2019WR026951, 2020.

Zink, M., Kumar, R., Cuntz, M., and Samaniego, L.: A high-resolution dataset of water fluxes and states for Germany accounting for parametric uncertainty, Hydrology and Earth System Sciences, 21, 1769–1790, https://doi.org/10.5194/hess-21-1769-2017, 2017.